Clin Exp Metastasis (2012) 29:217–227
DOI 10.1007/s10585-011-9444-2

RESEARCH PAPER

Generation and characterization of orthotopic murine models for endometrial cancer

Silvia Cabrera · Marta Llauradó · Josep Castellví · Yolanda Fernandez · Francesc Alameda · Eva Colás · Anna Ruiz · Andreas Doll · Simó Schwartz Jr. · Ramon Carreras · Jordi Xercavins · Miguel Abal · Antonio Gil-Moreno · Jaume Reventós

Received: 26 April 2011 / Accepted: 7 December 2011 / Published online: 25 December 2011

Abstract We describe the generation of two orthotopic murine models for endometrial cancer (EC).The first model is generated from endometrial Hec-1A cancer cells transfected with luciferase and injected directly into the uterus of female mice. This model allows a follow-up with bioluminescence imaging (BLI) along the experiment and generates abdominal dissemination and lymphatic and hematogenous metastases in high percentages, also detectables with BLI. The dissemination pattern of this model imitates the advanced stages of EC in patients, and its molecular profile corresponds to aggressive type 2 EC (p53 positive, hormone receptors negative, high percentage of Ki67 positive cells). The second model is derived from endometrioid human tissue collected from surgical pieces. By injecting this tissue inside the uterine cavity of a mouse we obtain orthotopic growth with pelvic dissemination and lymph node metastasis. The molecular pattern observed in human type 1 endometrioid EC (p53 negative, low Ki67 index, presence of hormone receptors) is conserved after the murine growth in orthotopic tumor and metastases. This model supposes a singular pre-clinical tool to study therapeutic agents, though it mimics clinical and molecular behavior of endometrioid EC, which is the most common histology in the patient.

Keywords Endometrial cancer · Animal model · Orthotopic model · Bioluminescence · Murine model

Abbreviations

EC	Endometrial cancer
BLI	Bioluminescence imaging
Hec1A	Human endometrial carcinoma 1A
Fluc	Firefly luciferase
Hec1A-Fluc	Hec1A cells transfected with luciferase gen
FIGO	International Federation of Gynecology and Obstetrics
i.p	Intraperitoneal
ROI	Region of interest

Silvia Cabrera, Marta Llauradó, Antonio Gil-Moreno and Jaume Reventós have contributed equally to this study.

Electronic supplementary material The online version of this article (doi:10.1007/s10585-011-9444-2) contains supplementary material, which is available to authorized users.

S. Cabrera (✉) · J. Xercavins · A. Gil-Moreno
Unit of Gynecologic Oncology, Department of Gynecology, Hospital Vall d'Hebron, Passeig de la Vall d'Hebron 119, 08035 Barcelona, Spain
e-mail: silviacabreradiaz@hotmail.com; scabrera@vhebron.net

M. Llauradó · E. Colás · A. Ruiz · A. Doll · J. Reventós
Biomedical Research Unit, Vall d'Hebron Research Institute, Passeig de la Vall d'Hebron 119, 08035 Barcelona, Spain
e-mail: jreventos@ir.vhebron.net

J. Castellví
Department of Pathology, Hospital Vall d'Hebron, Barcelona, Spain

Y. Fernandez · S. Schwartz Jr.
CIBBIM-Nanomedicine, Hospital Vall d'Hebron, Barcelona, Spain

F. Alameda
Department of Pathology, Hospital del Mar, Barcelona, Spain

R. Carreras
Department of Gynecology, Hospital del Mar, Barcelona, Spain

M. Abal
Translational Oncology Laboratory, Instituto de Investigación Sanitaria de Santiago, Complexo Hospitalario Universitario Santiago de Compostela, Santiago de Compostela, Spain

ph/s	Photons/second
H&E	Hematoxylin and eosin
IHC	Immunohistochemical
ER	Estrogen receptor
PR	Progesterone receptor
MSH6	MutS homolog 6 gene
MSH2	MutS homolog 2 gene
MLH1	MutL homolog 1 gene
SEM	Standard errors of the mean
3D	Three-dimensional

Introduction

The crude incidence of endometrial carcinoma (EC) in the European Union is 16 cases/100,000 women per year (age range 13–24). The mortality rate is 4–5 cases/100,000 women per year [1]. Age-standardized incidence rates continue to rise in most developed countries. Therefore, interest has been expressed in seeking new therapeutic agents, which either alone or in combination would allow improvement in the progression to disease free and overall survival of women with this disease [2, 3]. Type 1 EC represents a majority of the sporadic cases of EC, accounting for 70–80% of all new cases. These cancers are typically of endometrioid histology, and they are primarily associated with unopposed estrogen exposure. Type 1 endometrioid lesions arise in a background of hyperplasia and commonly express estrogen and progesterone receptors. Clinically, type 1 EC most often includes low-grade tumors with a favorable prognosis. In contrast, type 2 EC is less common, accounting for 10–20% of EC cases. These are often of a non-endometrioid, high-grade histology, usually papillary serous or clear cell. Type 2 EC is unrelated to estrogen exposure and typically arises in a background of atrophic endometrium. These cases are marked by a more aggressive clinical course with early spreading and poor prognoses [4]. Aside from their morphological and clinical features, type 1 and type 2 ECs are further distinguished by molecular alterations. Endometrioid and non-endometrioid ECs are associated with mutations of independent sets of genes [5, 6]. Endometrioid EC involves mutations in PTEN, K-ras, and β-catenin, as well as defects in DNA mismatch repair. Non-endometrioid EC frequently shows aneuploidy and p53 mutations [7, 8].

Notwithstanding the good prognosis of EC, myometrial infiltration and, particularly, distant metastases are its most devastating aspects. Approximately 25% of the patients who have undergone surgical staging are found to have extra-uterine disease [9]. EC spreads primarily to the pelvic and para-aortic lymph nodes, as well as to the adnexa and pelvic viscera. Distant metastases via the hematogenous route have a low incidence. Even so, pulmonary metastases have been reported to be one of the most common types of distant metastasis stemming from EC, and its incidence ranges from 2.3 to 4.6% [10, 11]. In EC, the precise molecular events that occur during the development, progression, invasion and metastasis generation are uncharacterized. To better understand the EC molecular mechanisms and to improve clinical treatment, the use of clinically relevant mouse models, which fulfill tumor progression, invasion and metastases, is an essential requirement. Our group has been working on the development of subcutaneous and orthotopic murine models in EC [12], and the main limitation we have encountered has been the difficulty in performing an in vivo follow-up on the models. Therefore, we have focused on the implementation of new tools, in order to resolve this handicap, especially through the use of bioluminescence imaging (BLI), a new technique that monitors and quantifies tumor growth, progression and metastases development, as well as response to therapy in a non-invasive manner [13, 14].

The objective of the present study is to present our results in the generation of two new orthotopic mouse models for EC, which are reproducible and imitate the infiltrative process and metastatic behavior of EC. By their development, we are able to provide an advanced tool for future studies dealing with tumoral physiopathology and the development of anti-cancer therapies.

Materials and methods

Cell line constructs and stable cell line generation

Human endometrial carcinoma 1A (Hec1A) cell line was cultured as described in Doll et al. [12]. Plasmid construction consisted of the full-length luciferase gene (firefly luciferase cDNA), which was inserted at the *Hin*dIII/*Xba*I position of the pcDNA3.1 vector (Invitrogen, Carlsbad, CA). The correct orientation and the reading frame were confirmed by sequencing. Then, Hec1A cells were transfected with the newly constructed plasmid pcDNA3.1-firefly luciferase (Fluc) using Lipofectamine™ 2000 (Invitrogen). Hec1A-Fluc stably expressing cells were selected with 350 μg/ml hygromycin B (Invitrogen). To validate the bioluminescent light production of the clones, we tested them by in vitro BLI assay using IVIS® Spectrum (Caliper Life Sciences, MA).

Cell proliferation assay

Cell proliferation assays were performed using the CellTiter 96® AQueous One Solution (MTS) (Promega, Biotech Ibérica, Madrid, Spain), which is a colorimetric method for determining the number of viable cells in proliferation. 5×10^3 cells (for the non transfected Hec-1A cell line and

clones 4, 5, 8 and 9 of the transfected Hec-1A-Fluc cells) were plated in triplicate on p96 plates in complete medium (10% FBS) and incubated 48 h. Measurements were made according to the manufacturer's protocol.

Transwell invasion assay

Cell invasion assays were performed using the Cyto-SelectTM 24-Well Cell Invasion Assay kit, Fluorimetric Format (CBA-101-C; Cell Biolabs, Inc, San Diego, CA, USA). 0.5×10^6 cells (for the non transfected Hec-1A cell line and clones 4, 5, 8 and 9 of the transfected Hec-1A-Fluc cells) were plated without serum media in triplicate and were allowed to invade towards supplemented media during 48 h. Cells were quantified according to the manufacturer's protocol.

Endometrial tumor samples

Two tumor samples were obtained from surgical pieces collected from EC staging surgeries performed in the Gynecologic Oncology Unit of the Hospital Vall d'Hebron. Patients gave their informed consent before the surgical procedures. The fresh uterine tissue was evaluated by a pathologist, who indicated the best zone from which to extract a viable tumoral piece. The two selected endometrial tumor samples corresponded to endometrioid EC with histologic grade 2, in surgical stage IA for patient A and II for patient B by 2009 International Federation of Gynecology and Obstetrics classification (FIGO).

Animals

Six-week old female athymic nude mice (Charles River Laboratories, Inc., Wilmington, MA) were used in this model. The animals were housed in individually ventilated cage units and were maintained under pathogen-free conditions. Food and water were provided ad libitum. Specific pathogen-free conditions were respected during the surgery and the follow-up for the animals. The animals were sacrificed for necropsy by cervical dislocation after sedation. All the procedures regarding experimentation and animal care were performed according to the guidelines of the Spanish Council for Animal Care and the protocols of the Ethics Committee for Animal Experimentation of our Institution.

Orthotopic EC models

We generated two different orthotopic EC models by using the two types of samples described above (the Hec1A-Fluc cell line and the human endometrioid cancer tissue) and by testing two inoculation techniques (transmyometrial and transvaginal). Mice were anesthetized with 2% isofluorane (ABBOT Laboratories, Madrid, Spain), and the lower abdomen was swabbed with 70% alcohol. A longitudinal incision (medial laparotomy) was performed and the murine uterus was exposed. EC cells or tissue were indistinctly inoculated into the uterine body and the uterine horns. Since implantation inside the endometrial cavity was the main objective in the generation of this model, both transvaginal and transmyometrial inoculation techniques were studied.

Orthotopic endometrial tumor model derived from cell line

For transmyometrial inoculation, 1×10^6 of Hec1A-Fluc cells resuspended in 50 µl of Matrigel (BD Matrigel™ Basement Membrane Matrix, BD Biosciences, San Jose, CA) were injected directly into the endometrial cavity through the myometrium. A 27G insulin syringe (Myjector® 1 ml, Terumo, Somerset, NJ) was used for the injection. The strain on the endometrial cavity and the expulsion of a small quantity of fluid through the vagina ensured the correct localization of the injection.

For transvaginal inoculation, 1×10^6 of Hec1A-Fluc cells in 50 µl of Matrigel were introduced transvaginally by means of an Abbocath®24G (ABBOCATH®-T, Venisystems™, Hospira Inc, Lake Forest, IL). Laparotomy and exposure of the uterus were performed, in order to control the intrauterine localization of the tip of the catheter. The strain on the endometrial cavity ensured the intrauterine inoculation of the cell suspension.

Orthotopic endometrial tumor model derived from human tissue samples

A tissue sample of 1 mm^3 was collected from the surgical piece and immediately implanted into the sub-scapular region of a previously anesthetized mouse, in order to generate a subcutaneous model to check the viability of the tissue and to amplify the tumoral volume. To achieve our orthotopic models, we needed a tumor volume of about 1–1.5 cm^3 per mouse. This tumoral piece was mechanically crumbled and injected transvaginally or transmyometrially following the previously described procedure. Since the implants in this model were not completely liquid, the needles employed to inoculate the mice had to be thicker. A 23G syringe (BD Microlance™ 3, 23G × 1″-Nr. 16) was used to generate the transmyometrial model, and an intravenous Catheter 18G Biovalve (Vycon, Ref. 106.12, 1.2 mm diameter, Ecouen, France) was used to generate the transvaginal one.

BLI of the cell line derived model

In vivo BLI

D-Luciferin substrate (Promega Biotech Ibérica, Madrid, Spain) at 150 mg/kg was injected intraperitoneally (i.p.) two minutes before animal sedation. Mice were placed inside the imaging chamber, and images were taken every 2 min, up to 20 min, to determine the D-luciferin kinetics of our model, which would define the suitable time it would take to get the images and compare the results over time. We imaged our model at an 8–13 min range after D-luciferin injection. Image acquisition conditions were modified during the experiment as needed. The first control of the Hec1A-Fluc orthotopic model was carried out 2–5 days after the surgical implantation of the transfected cells. This was done to ensure that there had been no spillage of tumoral cells during the intrauterine injection, which may have caused abdominal implants not to have adequate orthotopic infiltration, and also to check for the presence of pelvic signals. Subsequently, imaging was performed weekly up to six weeks to evaluate the orthotopic tumor growth and metastatic dissemination. The brightest abdominal signals were shielded, in order to detect and quantify weaker signals in the thoracic region. The light emitted from the bioluminescent cells was detected in vivo by the IVIS® Spectrum, digitalized and electronically displayed as a pseudo color overlay onto a gray scale animal image. Regions of interest (ROIs) from displayed images were drawn automatically around the primary tumor and metastatic bioluminescent signals and quantified as calibrated units photons/second (ph/s). The auto ROIs were draw along time using the same ROI parameters (threshold = 20%, lower limit = 1.0 and minimum size = 20).

Ex vivo BLI

At day 47, 10 min before necropsy, all of the mice were i.p. injected with a D-luciferin substrate. During necropsy, a macroscopic evaluation was performed. Organs were obtained in the following order: brain, axillary lymph nodes, lungs, mediastenial and inguinal lymph nodes, peritoneum, uterus-adnexa and pelvic fat, para-aortic and mesenteric lymph nodes, pancreas, spleen, kidneys, liver, and diaphragm. Each organ was collected and immersed in a D-Luciferin 300 μg/ml PBS and maintained in cold conditions until ex vivo BLI was performed using the IVIS® Spectrum. Immediately after, the tissues were cleaned with PBS (1×) and introduced into a 3.7–4% formaldehyde solution, in order to fix them and perform the histological analysis.

Histological examination

All tissues were formalin-fixed and processed for routine histological examination. Hematoxylin–Eosin (H&E) staining was performed on 24 h formalin-fixed paraffin-embedded 4 μm sections using routine histological procedures. Histological examination was carried out by an experienced pathologist.

Immunohistochemical (IHC) analysis

Formalin-embedded sections from primary and metastatic tumor tissue were mounted on glass slides, fixed in acetone and air-dried. The following antibodies were used for tissue staining: Estrogen Receptor (1D5, Dako, Glostrup, Denmark) 1:50; Progesterone Receptor (Pgr636, Dako), 1:200; Ki-67 (MIB-1, Dako), 1:100; E-cadherin (NCH-38, Dako), 1:50; β-catenin (β-Catenin-1, Dako), 1:100; p53 (DO7, NovoCastra Lab., NewCastle,UK), 1:50; MSH6 (MSH6 44, BD Transduction, Franklin Lakes, NJ), 1:40; MSH2 (G219-1129, BD Transduction), 1:400; MLH1 (G168-15, BD Transduction) 1:40. Staining was performed as described in the customer instruction manual. All stainings were semi-automated and performed on an Autostainer Link 48 (Dako) using the flex Dako detection system, as recommended by the manufacturer. The deparaffinized tissue sections were treated with heat prior to the IHC staining procedure for epitope retrieval, using a PTLink Dako System by immersion of tissue sections in citrate buffer pH 6.0 (ER, Ki67, β-catenin) or pH 9.0 (the other antibodies) in an autoclave at 95°C for 20 min. IHC analysis was performed by an experienced pathologist. The percentage of tumor cells expressing each molecular marker was assessed.

Statistical analyses

The mean BLI intensity, mean tumor volume, and corresponding standard errors of the mean (SEM) were determined for each experiment. Nonlinear regression plots were used to describe the relationship between BLI intensity and time after cell injection; R^2 values were reported to assess the quality of the nonlinear regression model. All of the analyses and graphs were completed using GraphPad Prism 5 software.

Results

In vitro analysis of the Hec-1A-Fluc clones

To obtain Hec-1A light-producing cells for the generation of the orthotopic Hec-1A EC mouse model, stable transfection

of the full-length luciferase gene (Fluc) into the Hec-1A cells was performed. Stable transfected Hec-1A-Fluc cells were established, and single clones were isolated and maintained in cell culture. Prior to the selection of the final clone, the morphology of the different clones were checked, however, we did not observe any difference. Moreover, to examine the behavior between the different Hec-1A-Fluc clones in vitro experiments of proliferation and invasion were performed. The results showed that both morphology and behavior of the different single clones and the non transfected cell line were similar (Supplementary Fig. S1). Hence, we believe that independent clones might perform in a similar manner when used in in vivo experiments. The production of light for each clone was assessed by in vitro BLI assay using IVIS® Spectrum (Caliper Life Sciences). The efficiency of light emission for each clone was linear, being proportional to the number of cells plated. Finally, the Hec1A-Fluc clone five with the highest light emission was selected for the in vivo experiments.

Efficiency of inoculation techniques in the generation of murine models

Two different approaches to inoculate Hec1A-Fluc EC cells into mouse uteri were compared, transvaginal and transmyometrial ($n = 8$ per group). In the transmyometrial group, six mice (75%) developed orthotopic tumors and all of them presented metastatic spread in the pelvic cavity, as well as lymph node metastasis. Hematogenous metastases in the lung were observed in four mice. In the transvaginal group, only one mouse (12.5%) developed an orthotopic tumor and pelvic and lymph node metastases (Table 1). From these results we concluded that the transmyometrial inoculation procedure is more efficient than the transvaginal method in generating orthotopic endometrial tumors and metastases.

Table 1 Comparative results of transmyometrial and transvaginal inoculation techniques in Hec1A cell line derived model

	Inoculation tecnique	
	Transmyometrial	Transvaginal
Mice used, *n*	8	8
Mice with endometrial tumor, *n*	6	1
Tumor incidence, %	75%	13%
Metastasis incidence, %		
Pelvic implants	6/6 (100%)	1/1 (100%)
Lymph node metastasis	6/6 (100%)	1/1 (100%)
Abdominal implants	5/6 (83%)	0/1 (0%)
Lung metastasis	4/6 (66%)	0/1 (0%)

Orthotopic cancer development and metastasis generation in Hec1A-Fluc murine models

Seventeen nude mice were inoculated with Hec1A-Fluc cells using the transmyometrial technique. In the first in vivo BLI performed at day 5, 16 of the mice presented orthotopic pelvic signals, and no abdominal cell spread was observed. During the follow-up, two mice were discarded: one because it had not developed any orthotopic signals 19 days after inoculation, and the other because of renal failure at day 18. In the necropsy and histological study of this last mouse, we observed that it presented an endometrial tumor, though no metastasis was detected.

Thus, 15 mice were successfully monitored during the whole experiment. In vivo BLI images of orthotopic tumor growth and metastatic lesions of a representative mouse over time are shown in Fig. 1a**.** BLI signals were quantified over time (Fig. 1b). An exponential increase of orthotopic BLI signals that correspond to endometrial tumor growth and pelvic metastases was observed over time. At the end of the experiment (day 47), mice were euthanized and ex vivo BLI analysis was performed. The organs were subsequently fixed and H&E stained (Fig. 2).

Sixteen of the 17 mice (94%) generated endometrial tumors. 87% of the mice presented pelvic implants in the pelvic peritoneum, bladder or prevesical fat. Lymphatic dissemination was observed in 93.3% of the animals. Para-aortic lumbar lymph nodes were affected in 100% of these mice, which means that this was the first nodal station for the uterine tumors in these mice. Other affected lymph nodes were: para-aortic renal (86%), mediastenial (36%), mesenteric (29%), inguinal (14%) and axillary (7%). Abdominal implants were detected in 80% of the mice affecting the pancreas, liver, spleen, kidneys, diaphragm and abdominal peritoneum. Hematogenous metastases in the lungs were detected in 73% of the animals, but no intrahepatic metastases were observed in our series. Table 2 summarizes the orthotopic endometrial primary tumors and the metastases generated.

Orthotopic cancer development and loco-regional dissemination in endometrioid murine models

We inoculated 10 mice transmyometrially with two human endometrioid tumoral samples (five animals per sample), which had been previously grown subcutaneously. As the follow-up was performed by abdominal palpation and weight control, mice were sacrificed when they presented pelvic masses or ascites. The mean time before necropsy was 62.7 days (range 58–66). Organs were fixed and H&E stained. Nine mice (90%) developed endometrial tumors, which maintained a histological pattern similar to the original endometrioid endometrial tumor. Myometrial

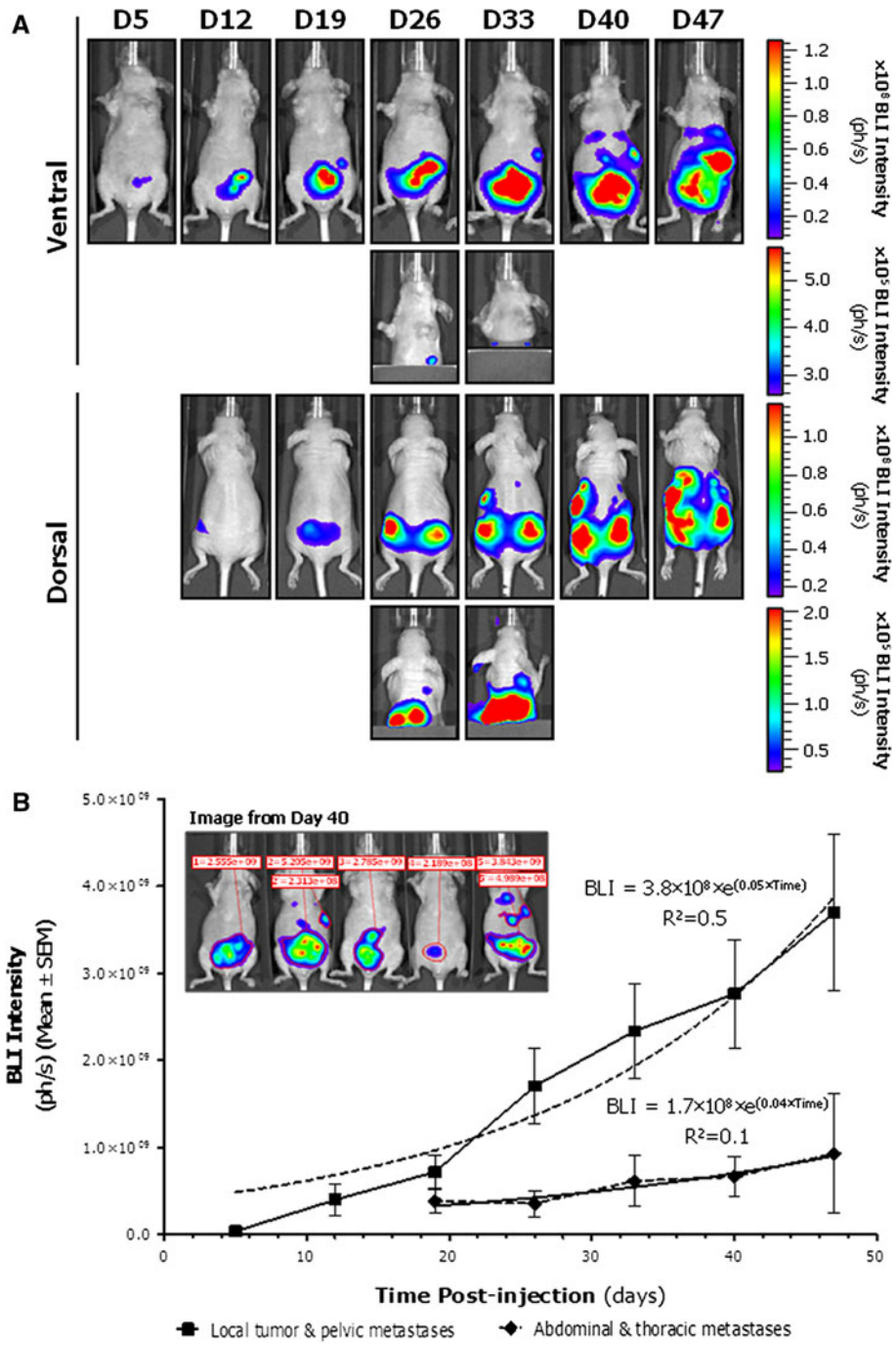

Fig. 1 In vivo BLI of the orthotopic Hec1A murine model. Hec1A-Fluc cells were directly injected into the endometrial cavity. Images were taken once a week for 7 weeks. **a** Selected ventral and dorsal view images from one representative mouse are shown. To check for metastases development into the upper part of the mouse, animals were imaged with the primary tumor shielded. Images from each corresponding view were set at the same pseudocolor scale to show relative BLI changes over time. **b** Primary tumors and locoregional metastasis growth rate from the ventral abdominal region was quantified weekly by means of BLI intensity (ph/s). A region of interest (ROI) for each animal ($n = 15$) was defined at every time point, and mean values ± SEM are displayed over time. The dotted line indicates the non-linear regression fits of the exponential metastatic growth

infiltration was observed in all of these mice, and infiltration developed from the inside to the outside of the uterus, as happens in patients. 77% of the mice presented dissemination in the pelvic cavity, and 66% also had abdominal implants. Lymph node metastases were observed in one mouse. No hematogenous metastasis was found in this series. All of the mice that presented extrauterine dissemination also developed hemorrhagic ascites (Table 3).

IHC analysis shows two different molecular patterns resembling the molecular characteristics of type 1 and type 2 EC

Globally, p53, ER, PR, Ki67, MSH6, MSH2 and MLH1 showed nuclear expression. E-cadherin was expressed in the membrane and β-catenin in membrane and weakly in cytoplasm. The intensity of the staining was homogeneous in all tumor cells of each sample. The Hec1A tumor molecular

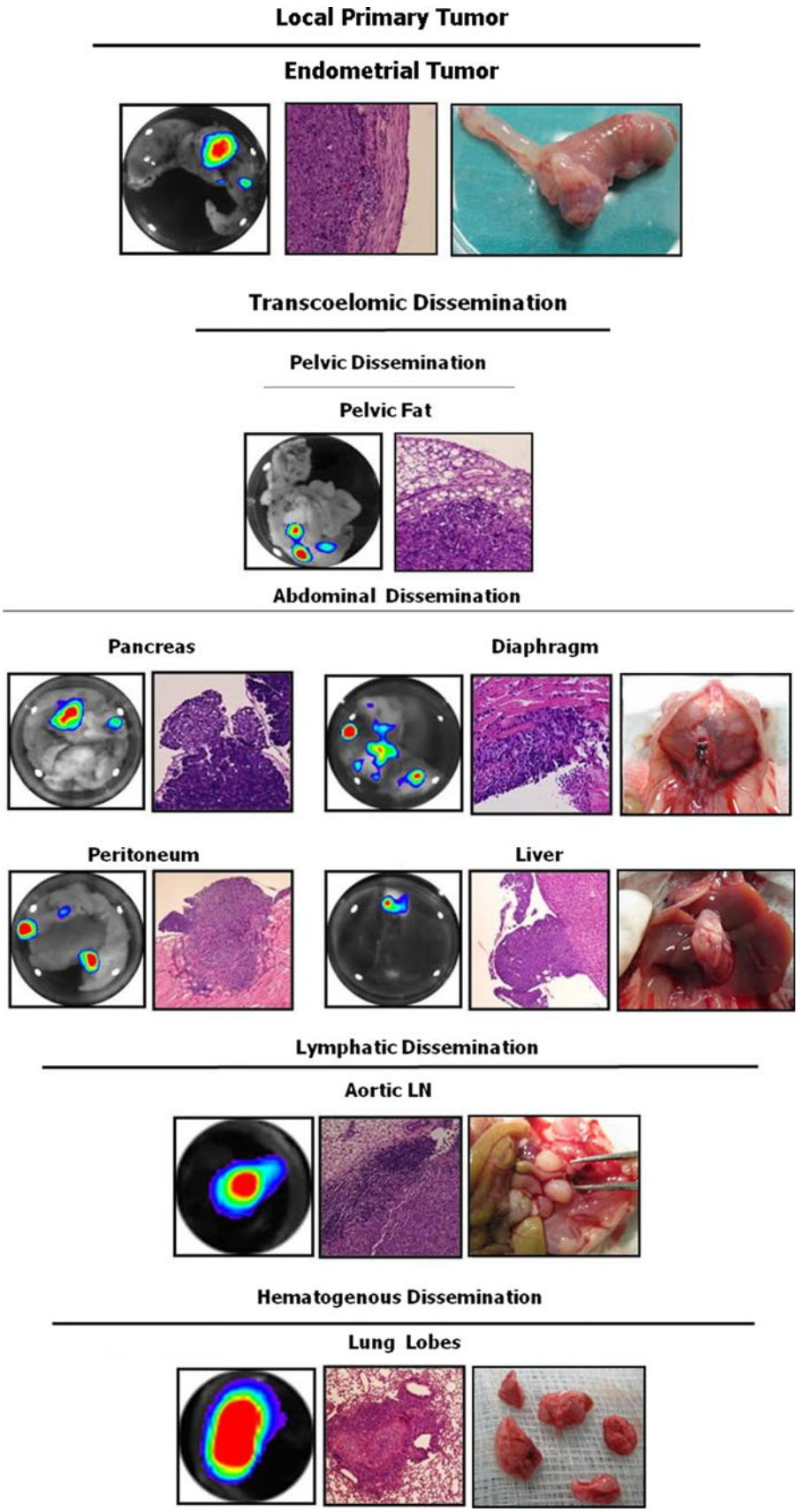

Fig. 2 Ex vivo bioluminescence images, H&E staining and necropsy images of the orthotopic Hec1A endometrial tumor-bearing mice, showed: Endometrial tumor. H&E staining confirmed the endometrial generation of the tumor and the infiltration of myometrium from inside to outside the uterus, as happens in patients, pelvic and abdominal spread, para-aortic lymph node dissemination, and hematogenous metastasis, showing macroscopic lung metastasis

Table 2 Results of transmyometrial generation of orthotopic murine model derived from Hec1A-Fluc cell line

Mice used, *n*	17
Mice with endometrial tumor, *n*	16
Tumor incidence, %	94%
Mice finally analysed[a], *n*	15
Metastasis incidence, %	
Pelvic implants	13/15 (87%)
Lymph node metastasis	14/15 (93%)
Para-aortic lumbar nodes	14 (100%)
Para-aortic renal nodes	12 (86%)
Mediastenial nodes	5 (36%)
Mesenteric nodes	4 (29%)
Inguinal nodes	2 (14%)
Axillary nodes	1 (7%)
Abdominal implants	12/15 (80%)
Pancreas	12 (100%)
Liver	11 (92%)
Spleen	11 (92%)
Kidneys	11(92%)
Diaphragm	11 (92%)
Peritoneum	10 (83%)
Lung metastasis	11/15 (73%)

[a] One mouse was killed at day 18 because of acute renal failure and anasarca

Table 3 Results of transmyometrial generation of orthotopic murine model derived from endometrioid tissue samples

Mice used, *n*	10
Mice with endometrial tumor, *n*	9
Tumor incidence, %	90%
Metastasis incidence, %	
Pelvic implants	7/9 (78%)
Lymph node metastasis	1/9 (11%)
Abdominal implants	6/9 (67%)
Lung metastasis	0/9 (0%)

profile was representative of an undifferentiated and more aggressive endometrial tumor (p53 positive, hormone receptors negative, high percentage of Ki67 positive cells), similar to type 2 EC. The endometrioid molecular profile was representative of a more differentiated tumor (p53 negative, low Ki67 index, presence of hormone receptors). Hormone receptors varied depending on the original samples. In the sample from patient A, both estrogen and progesterone receptors were expressed, while only progesterone receptors were observed in the sample from patient B. This fact demonstrates a correlation in molecular behavior between the original human tissue sample and the tissue after growth in a mouse. The molecular pattern was also similar in the primary and metastatic tumors (Table 4; Fig. 3).

Discussion

Experimental models based on human EC cells have been widely described [15–18], mainly using subcutaneous xenografts. Although there is evidence that these models can predict clinical efficacy, they still have significant limitations, the most important of which is the different microenvironment of the tumoral implant from its original location. These limitations can lead to a low tumor blood supply that can produce central necrosis, an absence of tumoral infiltration and encapsulation, and more importantly, a lack of metastatic behavior [12]. Nonetheless, such models have helped us to understand the biology of tumors and have lead to some therapeutic approaches to human cancer. However, their handicaps have revealed to us the importance of developing a viable animal model that mimics the clinical behavior of cancer. Orthotopic injections of human cancer cells have been tested in different cancers, such as colon, lung, pancreas, bladder, stomach, and breast, among others [19–21]. These models have permitted the study of the metastatic process, although one of their most important disadvantages is the in vivo follow-up. The development of different strategies has been introduced, in order to monitor orthotopic tumor growth and detect the appearance of metastasis. In this respect, BLI represents a useful tool to resolve this handicap, effectively monitoring disease progression as it happens.

Our study generates and characterizes two new orthotopic models for EC, which closely reflect the clinical behavior of this illness in patients. Using Hec1A-Fluc cells, intrauterine implantation mimics the process of EC development, myometrial infiltration and metastasis generation. The use of the intrauterine injection technique represents an advantage over our previously characterized mouse model [12], because the implant follows the natural infiltrative process from inside to outside the uterus. Moreover, in vivo BLI has enabled the direct observation of cancer cells spreading from their site of origin and arriving at secondary sites, longitudinally in time. In vivo BLI also offers early reads on disease progression and a rapid, sensitive and less invasive way to monitor tumoral growth and metastases. 80% of our mice developed advanced disease with lymphatic, intra-abdominal and/or hematogenous metastasis, which would represent stage IV in the FIGO classification for EC [22]. Our results showed a strong correlation between orthotopic tumor development and the appearance of metastasis, as 14 of the 15 mice presented metastasis. The molecular pattern of this model corresponds to a more aggressive and undifferentiated tumor similar to type 2 EC.

Previously, Kamat et al. [23] described an orthotopic EC model derived from Ishikawa and Hec1A cell lines transfected with luciferase. In vivo BLI was performed only

Table 4 Percentage of positive cells in the inmunohistochemical analysis of primary and metastasic samples in Hec1A and human endometrioid derived murine models

	p53	ER	PR	β-catenin	Ki67	E-cadherin	MSH2	MLH1	MSH6
HEC-1A									
Primary Tumor (uterus)	100%	0	0	100%	100%	100%	100%	100%	100%
Metastasis (lung)	100%	0	0	100%	100%	50%	100%	100%	100%
Metastasis (para-aortic lymphnode, PAN)	100%	0	0	80%	90%	50%	100%	100%	100%
Endometrioid adenocarcinoma									
Pateint A									
Primary Tumor (uterus)	0	40%	40%	100%	50%	100%	0	0	5%
Metastasis (peritoneal implant)	0	40%	40%	80%	50%	100%	0	0	5%
Pateint B									
Primary Tumor (uterus)	0	0	50%	100%	2%	0	0	0	80%
Metastasis (peritoneal implant)	0	0	60%	80%	2%	0	0	0	80%

twice during the experiment, mainly to ensure correct cell injection. Both models produced metastatic implants to the peritoneum, bowel mesentery, lymph nodes, kidney, and liver. In our study, we fully describe and better characterize the orthotopic EC model by using a lower number of cells (1×10^6 instead of 4×10^6) over a similar period of time. This fact produced less explosive tumoral growth and more progressive metastatic appearance, making this model more useful for therapeutic schemes, since there was a well-defined time between the cell implantation and the appearance of metastasis. By performing BLI weekly throughout the course of the experiment, we were able to follow all disease progression, including the orthotopic tumor growth and the metastatic dissemination to distant organs.

A similar orthotopic model derived from injection of Hec-1A, Ishikawa or SPEC-2 cells into the murine uterine horn was published by Lee et al. [24]. A higher quantity of cells resuspended in Hank's Balanced Salt Solution (HBSS; Invitrogen) instead of Matrigel was used. Given that the main goal of their publication was to perform a therapeutic trial they do not describe the tumor and metastasis incidence. Luciferase for BLI follow-up is not used, and they do not molecularly characterize the tumor or the implants to determine their molecular profile.

A more recent model has been described by Takahashi et al. [25] in a study in which a highly metastatic model was needed. To generate a peritoneal dissemination endometrial model Hec1A tumor cells were intraperitoneally injected into nude mice. To develop a lymph node metastasis model tumor cells were injected into the uterine cavity of laparotomized mice, and to develop a lung metastasis model cells were injected into the tail vein of nude mice. In contrast, in the model that we describe the process of metastatic development derives from the myometrial infiltration and lymph-vascular invasion of the orthotopic implant, as happens in the patient. Therefore, we can study the different molecules implicated in infiltration and lymph-vascular invasion, which are essential steps in metastatic development.

Our model is easy to generate, rapid in orthotopic development and metastasis generation, and it is easily monitored by BLI technology, while also being clinically representative of advanced disease. This means that it represents an advance in future, preclinical studies of EC, since it shows all of the phases of the disease: cancer generation inside the uterine cavity, myometrial infiltration and lymph-vascular invasion, peritoneal dissemination, and lymphatic and hematogenous metastasis.

Moreover, we have developed a second orthotopic EC model using human tumoral tissue, in order to keep the molecular phenotype and 3D structure. This type of model has never been described before in the literature. Orthotopically implanted, human endometrioid tissue produces myometrial infiltration, lymph-vascular invasion and dissemination in pelvic cavity. It maintains the molecular and histological characteristics of the original samples, reproducing glandular patterns and expressing hormone receptors. This model could be complementary to the Hec1A cell line model for testing new anti-cancerous drugs, since it presents endometrioid EC histology and immunophenotype.

In conclusion, we have generated and characterized two different orthotopic EC murine models that could be useful tools in preclinical studies. The Hec1A cell line derived model represents advanced disease and can be used to test the efficacy of anti-metastatic drugs. The human tissue derived model maintains the histological endometrioid pattern of the original tumor and represents local and locally-advanced disease. It can be used to specifically test drugs against endometrioid EC. Finally, both models could be useful for studying how the process of metastatic appearance is influenced by gene expression.

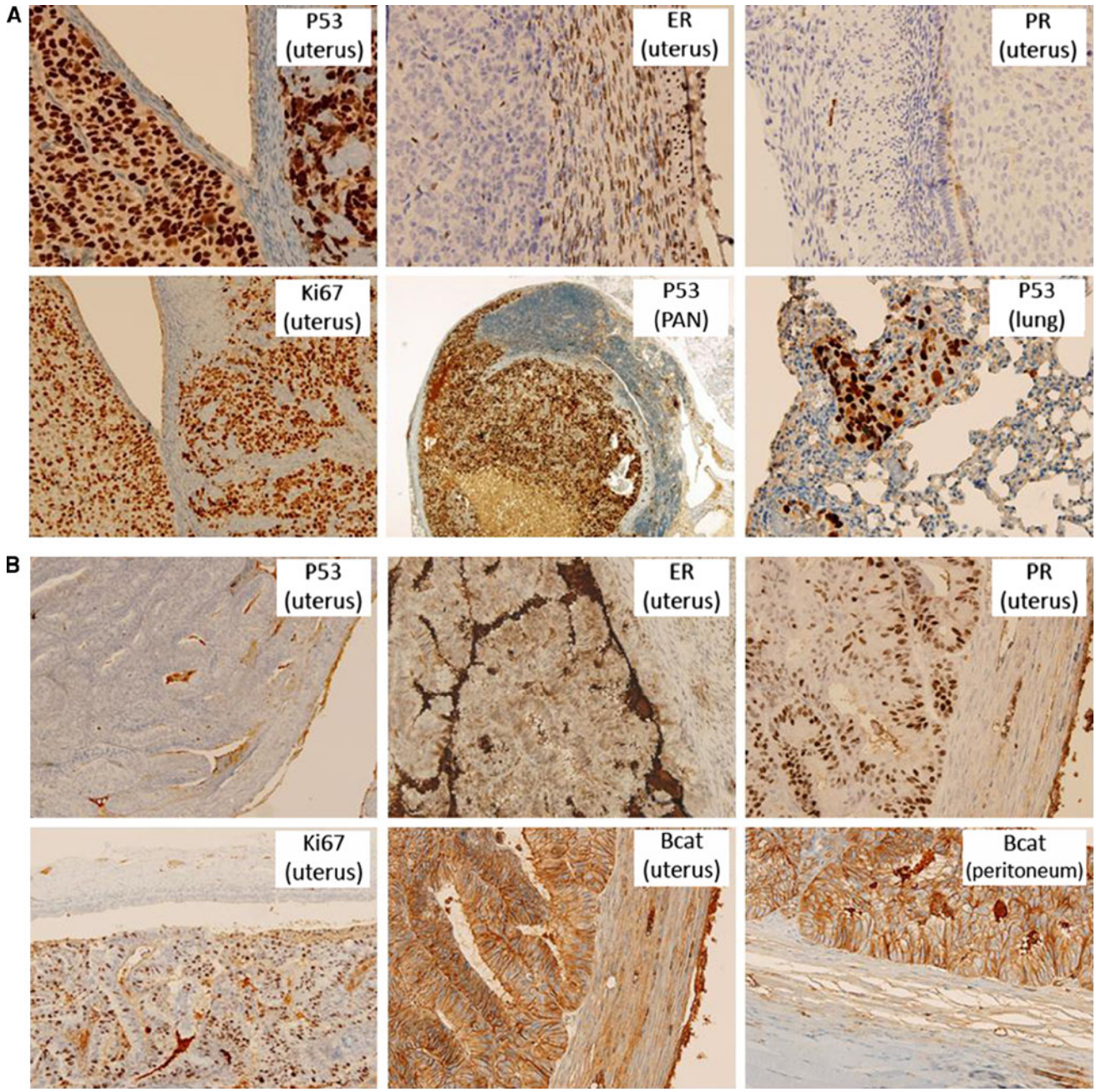

Fig. 3 Immunohistochemical characterization of the orthotopic mouse models. **a** Images of the Hec-1A cell line derived model showed positivity to p53, Ki67 with high expression and negativity to progesterone and estrogen receptors as type 2, non-endometrioid EC. **b** Immunohistochemical images of the tissue derived model, showed glandular structure with negativity to p53 and positivity to progesterone and estrogen receptors as endometrioid, low grade EC. *ER* estrogen receptors, *PR* progesterone receptors, *Bcat* β-catenin, *PAN* para-aortic lymph node

Acknowledgments The authors would like to thank Lisa Piccione for correction of the manuscript. This work has been supported by the Spanish Ministry of Science and Innovation (SAF 2005-06771; SAF 2008-03996; SAF 2010-10635-E; SAF2011-26548), the Spanish Ministry of Health (RTICC RD06/0020/0058, RD06/0020/1034; CP08/00142; PI08/0797), the Catalan Institute of Health (DURSI 2005SGR00553) and the Department of Universities and Research, Catalan Government (2009SGR00487, 2005SGR00553), the ACCIO program (RDITSCON07-1-0001), the Foundation La Marato de TV3 (grant 050431), the IV Grant Fundació Santiago Dexeus Font for Clinical Investigation Projects 2009, the National Programme of Biotechnology (FIT-010000-2007-26), and the European Commission Program Fondo Europeo de Desarrollo Regional (FEDER). M.LL. is recipient of a predoctoral fellowship from the Spanish Ministry of Innovation and Science (FI07/00423).

References

1. Baekelandt MM, Castiglione M (2009) ESMO Guidelines Working group.Endometrial carcinoma: ESMO clinical recommendations for diagnosis, treatment and follow-up. Ann Oncol 20(4):iv29–iv31
2. Homesley HD, Filiaci V, Gibbons SK et al (2009) A randomized phase III trial in advanced endometrial carcinoma of surgery and volume directed radiation followed by cisplatin and doxorubicin with our without paclitaxel: a Gynecologic Oncology Group study. Gynecol Oncol 112:543–552
3. Gehrig PA, Bae-Jump VL (2010) Promising novel therapies for the treatment of endometrial cancer. Gynecol Oncol 116:187–194
4. Bokhman JV (1983) Two pathogenetic types of endometrial carcinoma. Gynecol Oncol 15(1):10–17
5. Hecht J, Mutter GL (2006) Molecular and pathologic aspects of endometrial carcinogenesis. J Clin Oncol 24(29):4783–4791
6. Lax SF, Kendall B, Tashiro H et al (2000) The frequency of p53, K-ras mutations, and microsatellite instability differs in uterine endometrioid and serous carcinoma: evidence of distinct molecular genetic pathways. Cancer 88(4):814–824
7. Doll A, Abal M, Rigau M et al (2008) Novel molecular profiles of endometrial cancer-new light through old windows. J Steroid Biochem Mol Biol 108(3–5):221–229
8. Bansal N, Yendluri V, Robert M et al (2009) The molecular biology of endometrial cancers and the implications for pathogenesis, classification, and targeted therapies. Cancer Control 16(1):8–13
9. Vardi JR, Tadros GH, Anselmo MT et al (1992) The value of exploratory laparotomy in patients with endometrial carcinoma according to the new International Federation of Gynecology and Obstetrics staging. Obstet Gynecol 80:204–208
10. Ballon SC, Berman ML, Donaldson RC et al (1979) Pulmonary metastases of endometrial carcinoma. Gynecol Oncol 7:56–65
11. Bouros D, Papadakis K, Siafakas N et al (1996) Natural history of patients with pulmonary metastases from uterine cancer. Cancer 78:441–447
12. Doll A, Gonzalez M, Abal M et al (2009) An orthotopic endometrial cancer mouse model demonstrates a role for RUNX1 in distant metastasis. Int. J Cancer 125:257–263
13. O'Neill K, Lyons SK, Gallagher WM et al (2010) Bioluminescent imaging: a critical tool in pre-clinical oncology research. J Pathol 220:317–327
14. Zhang C, Yan Z, Arango ME et al (2009) Advancing bioluminescence imaging technology for the evaluation of anticancer agents in the MDA-MB-435-HAL-Luc mammary fat pad and subrenal capsule tumor models. Clin Cancer Res 15:238–246
15. Du X, Jiang T, Sheng X et al (2009) Inhibition of osteopontin suppresses in vitro and in vivo angiogenesis in endometrial cancer. Gynecol Oncol 115:371–376
16. Dai D, Holmes AM, Nguyen T et al (2005) A potential synergistic anticancer effect of paclitaxel and amifostine on endometrial cancer. Cancer Res 65(20):9517–9524
17. Saidi SA, Holland CM, Charnock-Jones S et al (2006) In vitro and in vivo effects of the PPAR-alpha agonists fenofibrate and retinoic acid in endometrial cancer. Mol Cancer 5:13
18. Wallace AE, Sales KJ, Catalano RD et al (2009) Prostaglandin F2A-F-prostanoid receptor signaling promotes neutrophil chemotaxis via chemokine (C-X-C Motif) Ligand 1 in endometrial adenocarcinoma. Cancer Res 69:5726–5733
19. Fidler IJ (1991) Orthotopic implantation of human colon carcinomas into nude mice provides a valuable model for the biology and therapy of metastasis. Cancer Metastasis Rev 10:229–243
20. John CM, Leffler H, Kahl-Knutsson B et al (2003) Truncated galectin-3 inhibits tumor growth and metastasis in orthotopic nude mouse model of human breast cancer. Clin Cancer Res 9:2374–2383
21. Chong L, Ruping Y, Jiancheng B et al (2006) Characterization of a novel transplantable orthotopic murine xenograft model of a human bladder transitional cell tumor (BIU-87). Cancer Biol Ther 5(4):394–398
22. Report Meeting (2009) The new FIGO staging system for cancers of the vulva, cervix, endometrium and sarcomas. Gynecol Oncol 115:325–328
23. Kamat AA, Merritt WM, Coffey D et al (2007) Clinical and biological significance of vascular endothelial growth factor in endometrial cancer. Clin Cancer Res 13:7487–7495
24. Lee JW, Stone RL, Lee SJ et al (2010) EphA2 targeted chemotherapy using an antibody drug conjugate in endometrial carcinoma. Cancer Res 16:2562–2570
25. Takahashi K, Saga Y, Mizukami H et al (2009) Cetuximab inhibits growth, peritoneal dissemination, and lymph node and lung metastasis of endometrial cancer, and prolongs host survival. Int J Oncol 35:725–729